Alternatively spliced mu opioid receptor C termini impact the diverse actions of morphine

Jin Xu,[1] Zhigang Lu,[2,3] Ankita Narayan,[1] Valerie P. Le Rouzic,[1] Mingming Xu,[1] Amanda Hunkele,[1] Taylor G. Brown,[1] William F. Hoefer,[4] Grace C. Rossi,[4] Richard C. Rice,[5] Arlene Martínez-Rivera,[5] Anjali M. Rajadhyaksha,[5] Luca Cartegni,[6] Daniel L. Bassoni,[7] Gavril W. Pasternak,[1] and Ying-Xian Pan[1]

[1]Department of Neurology and the Molecular Pharmacology Program, Memorial Sloan Kettering Cancer Center, New York, New York, USA. [2]Key Laboratory of Acupuncture and Medicine Research of Ministry of Education, and [3]First Clinical Medical College, Nanjing University of Chinese Medicine, Nanjing, China. [4]Department of Psychology, Long Island University, Post Campus, Brookville, New York, USA. [5]Division of Pediatric Neurology, Department of Pediatrics, Feil Family Brain and Mind Research Institute, Weill Cornell Medicine, New York, New York, USA. [6]Department of Chemical Biology, Ernest Mario School of Pharmacy, Rutgers, The State University of New Jersey, Piscataway, New Jersey, USA. [7]DiscoverX Corporation, Fremont, California, USA.

Extensive 3′ alternative splicing of the mu opioid receptor gene *OPRM1* creates multiple C-terminal splice variants. However, their behavioral relevance remains unknown. The present study generated 3 mutant mouse models with truncated C termini in 2 different mouse strains, C57BL/6J (B6) and 129/SvEv (129). One mouse truncated all C termini downstream of *Oprm1* exon 3 (mE3M mice), while the other two selectively truncated C-terminal tails encoded by either exon 4 (mE4M mice) or exon 7 (mE7M mice). Studies of these mice revealed divergent roles for the C termini in morphine-induced behaviors, highlighting the importance of C-terminal variants in complex morphine actions. In mE7M-B6 mice, the exon 7–associated truncation diminished morphine tolerance and reward without altering physical dependence, whereas the exon 4–associated truncation in mE4M-B6 mice facilitated morphine tolerance and reduced morphine dependence without affecting morphine reward. mE7M-B6 mutant mice lost morphine-induced receptor desensitization in the brain stem and hypothalamus, consistent with exon 7 involvement in morphine tolerance. In cell-based studies, exon 7–associated variants shifted the bias of several mu opioids toward β-arrestin 2 over G protein activation compared with the exon 4–associated variant, suggesting an interaction of exon 7–associated C-terminal tails with β-arrestin 2 in morphine-induced desensitization and tolerance. Together, the differential effects of C-terminal truncation illustrate the pharmacological importance of *OPRM1* 3′ alternative splicing.

Introduction

Most clinically used opiates, including morphine, act through the mu opioid receptor (1), producing both potent analgesia and a number of side effects, such as tolerance, physical dependence, constipation, respiratory depression, and addiction. The different responses to various mu drugs seen clinically (2, 3) and in animal models (4–6) suggested the existence of multiple mu opioid receptors, a concept initially proposed from classic pharmacological studies (7) and reinforced with the identification of an array of mu opioid receptor variants produced by alternative pre-mRNA splicing of the single-copy mu opioid receptor gene (*OPRM1*) (see review, refs. 8, 9).

Alternative splicing is commonly seen among G protein–coupled receptors (GPCRs) (10–12). However, the extensive alternative splicing of *OPRM1* is quite unusual, creating 3 structurally distinct classes of splice variants that are conserved from rodent to human: (a) full-length 7–transmembrane (7TM) C-terminal variants; (b) truncated 6TM variants that lack exon 1 and the first TM; and (c) truncated single TM variants containing the first TM (ref. 9 and Supplemental Figure 1; supplemental material available online with this article; https://doi.org/10.1172/JCI88760DS1). The relevance of the truncated variants has been extensively explored and validated (13–17), but few studies have examined the pharmacological consequences of alternative splicing of the C terminus in full-length 7TM variants.

Full-length 7TM C-terminal variants all contain the same 386-aa sequences in mouse and rat or 388-aa in humans that are encoded by *OPRM1* exons 1/2/3, but alternative splicing from exon 3 to various downstream exons produces unique alternative aa sequences at the tip of the intracellular C terminus. For example, the murine mu opioid receptor mMOR-1 has a C-terminal tail with 12 aa encoded by *Oprm1* exon 4, whereas the C-terminal tails in mMOR-1C and mMOR-1O contain 52 aa and 31 aa encoded by exons 7/8/9 and exons 7a/7b, respectively (8). Increasing evidence implies that the full-length 7TM C-terminal splice variants are pharmacologically important. At the mRNA level, they show region-specific expressions in rodents and humans (18–20), and long-term morphine treatment selectively increases C-terminal variant mRNA expression in various brain regions by as much as 300-fold (21). At the protein level, different C-terminal epitopes also differ in their cellular (i.e., pre- vs. postsynaptic) and regional distributions (22, 23). Additionally, heterodimerization of 7TM C-terminal variant mMOR-1D with gastrin-releasing peptide receptor has been implicated in morphine-induced itch (24).

▶ Related Commentary: https://doi.org/10.1172/JCI93582

Authorship note: J. Xu, Z. Lu, and A. Narayan contributed equally to this work.
Conflict of interest: The authors have declared that no conflict of interest exists.
Submitted: May 23, 2016; **Accepted:** January 12, 2017.
Reference information: *J Clin Invest*. https://doi.org/10.1172/JCI88760.

At the cellular level, all the 7TM C-terminal variants expressed in CHO cells bind [^{3}H][D-Ala^2,MePhe^4,Gly(ol)^5] ([^{3}H]DAMGO), a mu agonist, with high affinity and with only subtle differences in selectivity for the endogenous opioid peptides dynorphin A and β endorphin (18, 25, 26). However, in [^{35}S]GTPγS-binding assays, these C-terminal splice variants displayed marked differences in mu opioid–induced G protein coupling in both potency (EC_{50}) and efficacy (% of maximal stimulation) (26, 27), suggesting that the distal carboxyl terminal sequences influence mu agonist–induced receptor–G protein coupling and signal transduction. Multiple protein kinase phosphorylation sites are predicted from various alternative C-terminal sequences, and in vitro studies revealed differences in mu agonist–induced phosphorylation, internalization, and postendocytic sorting among several C-terminal splice variants (28, 29). However, in vivo functions of these C-terminal splice variants remain largely unknown.

The current study explores the functional significance of alternative C termini by generating 3 mutant mouse models with truncations of the distal end of the C terminus in 2 different inbred strains. By truncating either all C-terminal tails or selectively truncating C-terminal tails encoded by *Oprm1* exon 4 or exon 7, we now show the importance of these C-terminal tails in morphine tolerance, physical dependence, locomotor activity, and rewarding behavior, and suggest a role for exon 7–associated C terminus with β-arrestin 2 and morphine-induced desensitization and tolerance.

Results

Targeting intracellular carboxyl termini of the mu opioid receptors in mice. To target intracellular C-terminal tails that are generated through alternative splicing downstream from *Oprm1* exon 3 to the different downstream exons, we introduced a stop codon at the end or beginning of the targeted exon to produce 3 targeted mouse models without deletion of any individual exons (Supplemental Figure 1 and Supplemental Figure 2, A and B). The first mouse model (mE3M) was generated by inserting a stop codon at the 3′ end of *Oprm1* exon 3 that prevents translation of all exons downstream of exon 3, even though their mRNAs are expressed. Thus, the mE3M homozygous mice express only truncated mu opioid receptors lacking any distal C-terminal tails. In the other 2 mouse models (mE4M and mE7M), we introduced a stop codon at the 5′ end of *Oprm1* exon 4 or exon 7 to selectively terminate translation at the end of exon 3 only in exon 4– or exon 7–associated variants in mE4M or mE7M mice, respectively (Supplemental Figure 1 and Supplemental Figure 2, A and B).

All the stop codon mutations were introduced into W4 embryonic stem (ES) cells derived from 129/SvEv (129) or CY2.4 ES cells from C57BL/6J (B6) mice through homologous recombination using targeting vectors. Positive ES cells determined by Southern blot analysis were used to generate germ line–transmitting chimeras (Supplemental Figure 2C; see complete unedited blots in the supplemental material). WT and homozygous mice were produced through heterozygous breeding, identified by PCR restriction enzyme digestion (Supplemental Figure 2D) and confirmed by sequencing (Supplemental Figure 2E). The selection cassette (pgk-neo) was then removed by breeding with a *CAG-Cre* transgenic line to eliminate the potential influence of the cassette on transcription and splicing. As B6 and 129 mice have markedly different responses to mu opioids (30–32), we generated 2 sets of congenic mice for each mutant model on a B6 strain background (mE3M-B6, mE4M-B6, and mE7M-B6 WT and homozygous mice) and on a 129 strain background (mE3M-129, mE4M-129, and mE7M-129 WT and homozygous mice) by using traditional breeding combined with speed congenic breeding. Sequencing the exon-exon junctions of reverse-transcription PCR (RT-PCR) products from brain total RNAs confirmed that all the stop codon mutations were present, as expected (Supplemental Figure 2F). The WT control mice for each set of congenic lines and their corresponding homozygous mice were generated through heterozygous breeding and used for in vivo behavioral and ex vivo studies.

Expression of the mu opioid receptors in the targeted mouse models. To examine the effect of the stop codon mutations on mRNA expression, we quantified the mRNA levels of a number of splice variants in brains of the mutant mouse models using quantitative PCR (qPCR). The overall mRNA expression levels of the combined repertoire of full-length 7TM splice variants, determined by the primer set from exon 1 to exon 2 (mE1-2), failed to demonstrate significant differences in any of the mouse models regardless of the strain backgrounds (Supplemental Tables 1 and 2). Similarly, the mRNA levels of individual 7TM variants *mMOR-1A*, *mMOR-1D*, *mMOR-1I*, and *mMOR-1O*, 6TM variants *mMOR-1G* and *mMOR-1K*, and the single TM variants *mMOR-1S* and *mMOR-1R* were not appreciably altered in homozygous mice of all the models (Supplemental Tables 1 and 2). These results suggest that the stop codon mutations in mE3M, mE4M, and mE7M models did not have a generalized impact on their transcription and alternative splicing. However, the mRNA levels of *mMOR-1C* and *mMOR-1M* were greatly reduced in both the mE3M and mE7M mouse models. These reductions were probably due to nonsense-mediated mRNA decay, a process that degrades mRNA with a stop codon located more than 50 nucleotides upstream of the last exon-exon junction, because the stop codon insertions in the mE3M and mE7M models produce such a premature stop codon.

Protein expression of the full complement of 7TM variants was accessed by opioid receptor binding, recognizing that it measured the total pool of 7TM variants. Receptor expression levels are best assessed with antagonist binding, since the ligand labels both agonist and antagonist conformations to yield the full B_{max} (total density [concentration] in a sample of tissue) value. The maximal number of [^{3}H]naloxone-binding sites (B_{max}), an indicator of receptor protein expression, was significantly reduced in mE3M and mE4M homozygous mice on both 129 and B6 backgrounds (Table 1), but not in the mE7M mice. We observed no changes in binding affinity in either [^{3}H]naloxone saturation (Table 1) or competition studies with the mu agonists morphine, morphine-6-glucuronide (M6G), dynorphin A,and β-endorphin, and the antagonist naloxone against [^{3}H] DAMGO binding (Supplemental Table 3).

Effect of the C-terminal truncation on mu agonist–induced [^{35}S]GTPγS binding. The C terminus is critical for receptor–G protein interaction and signal transduction. To determine whether the C-terminal truncation alters mu agonist–induced G protein coupling, we examined DAMGO- and morphine-stimulated [^{35}S]GTPγS binding in whole brain membranes from the mutant mouse models. The truncations had little effect on ED_{50} values, but significantly reduced DAMGO- and morphine-induced maxi-

Table 1. Saturation studies using [^{3}H]naloxone

Mouse model	Genotype	[^{3}H]naloxone[A] K_D (nM)	[^{3}H]naloxone[A] B_{max} (fmol/mg protein)
mE3M-129	WT	0.63 ± 0.02	86.6 ± 7.9
	Mut	0.73 ± 0.09	57.4 ± 5.6[B]
mE3M-B6	WT	0.62 ± 0.06	58.9 ± 6.3
	Mut	0.66 ± 0.09	35.0 ± 5.2[B]
mE4M-129	WT	0.72 ± 0.02	86.0 ± 5.5
	Mut	1.48 ± 0.36[B]	61.2 ± 5.5[B]
mE4M-B6	WT	1.02 ± 0.36	64.6 ± 6.2
	Mut	0.99 ± 0.29	30.4 ± 9.4[C]
mE7M-129	WT	1.41 ± 0.33	81.8 ± 16.9
	Mut	1.21 ± 0.22	77.0 ± 7.3
mE7M-B6	WT	0.89 ± 0.05	64.0 ± 3.6
	Mut	0.99 ± 0.12	59.9 ± 6.9

[A][^{3}H]naloxone saturation studies were performed in membranes prepared from whole brains of indicated mouse models as described in Supplemental Methods. The K_D and B_{max} values were determined by nonlinear regression analysis (Prism). Results are shown as mean ± SEM of at least 3 independent determinations. [B]$P < 0.05$; [C]$P < 0.01$, compared with WT, 1-way ANOVA with Bonferroni's post hoc test. Mut, homozygous mice.

mal stimulation levels in mE3M and mE4M homozygous mice on both 129 and B6 backgrounds (Table 2), but not in mE7M-129 and mE7M-B6 homozygous mice, paralleling the changes in receptor expression (Table 1).

Effect of the C-terminal truncation on morphine analgesia. C-terminal truncation did not greatly affect morphine analgesia in naive animals in a radiant heat tail-flick assay (Table 3). There was a small shift in the ED_{50} values in the homozygous mE3M mice on both 129 and B6 backgrounds compared with their WT controls. However, these increases were far smaller than might be anticipated from the reduction in their receptor-binding sites (Table 1), suggesting spare receptors. A similar lack of correlation between the receptor density and analgesic response was previously observed in heterozygous mice from *Oprm1* KO mouse lines (33, 34).

Effect of the C-terminal truncation on morphine tolerance. Chronic morphine treatment (10 mg/kg, s.c. twice a day) induced modest tolerance in the respective WT B6 control mice from all mutant mouse models over 5 days (Figure 1A). However, tolerance developed faster and to a greater extent in truncated mE3M-B6 and mE4M-B6 homozygous mice. This enhanced tolerance was more evident in mE3M and mE4M homozygous mice on the 129 background. As previously reported (30, 35), little morphine tolerance developed in WT 129 control mice. In contrast, the truncated mutant mE3M-129 and mE4M-129 homozygous mice developed morphine tolerance to an extent similar to that seen in the WT B6 mice (Figure 1A). Cumulative dose-response curve studies before and after chronic morphine administration further confirmed these results (Figure 1B and Table 4). Chronic morphine markedly shifted the curves to the right and increased the ED_{50} values in both mE3M-129 and mE4M-129 homozygous mice, while the same morphine treatment did little in the respective WT 129 control mice.

Truncating exon 7–associated C-terminal tails in B6 (mE7M-B6 homozygous) mice had an opposite effect, with little change in morphine responsiveness over 5 days compared with that in the WT B6 littermate controls (Figure 1A). Cumulative dose-response studies revealed only a slight shift to the right in mE7M-B6 homozygous mice following chronic morphine (2.2-fold) compared with a significantly greater shift in WT B6 control mice (5.2-fold) (Figure 1B and Table 4). Since WT 129 mice showed little change with chronic morphine, it was not surprising to see that mE7M-129 homozygous mice also did not develop significant tolerance. Together, these results illustrate the divergent effects of exon 4– and exon 7–associated C-terminal tail truncations on morphine tolerance.

Effect of an antisense vivo–morpholino oligo targeting exon 7 inclusion on morphine tolerance and dependence in CD-1 mice. To further investigate the function of *Oprm1* exon 7–associated C-terminal variants in morphine tolerance and dependence, we used a knockdown strategy with an antisense vivo–morpholino oligo (ANT-vMO) that targets the intron/exon 7 junction to block splicing from exon 3 to exon 7, eliminating exon 7–containing transcripts. i.c.v. administration of the ANT-vMO in the CD-1 strain of mice effectively reduced *Oprm1* exon 3/7 splicing and downregulated exon 3/7–associated variant mRNAs, as determined by qPCRs, without significantly altering exon 1/exon 2– or exon 3/exon 4–containing transcripts (Figure 1C). The mismatch-morpholino oligo (MIS-vMO) or PBS was inactive. Mice treated with PBS or mis-morpholigo oligo displayed normal morphine tolerance after 5-day morphine treatment. However, mice treated with the ANT-vMO showed little morphine tolerance

Table 2. [^{35}S]GTPγS binding

Mouse model	Genotype	DAMGO EC_{50} (μM)[B]	DAMGO % Maximum stimulation[A]	Morphine EC_{50} (μM)	Morphine % Maximum stimulation
mE3M-129	WT	0.41 ± 0.1[B]	78 ± 3	0.22 ± 0.1	57 ± 3
	Mut	0.20 ± 0.1	49 ± 2[C]	0.28 ± 0.1	41 ± 5[C]
mE3M-B6	WT	0.37 ± 0.2	73 ± 3	0.22 ± 0.1	56 ± 5
	Mut	0.64 ± 0.3	39 ± 10[D]	0.18 ± 0.1	29 ± 9[D]
mE4M-129	WT	0.33 ± 0.1	74 ± 12	0.26 ± 0.1	51 ± 2
	Mut	0.36 ± 0.3	37 ± 3[D]	0.22 ± 0.1	38 ± 3[D]
mE4M-B6	WT	0.21 ± 0.1	66 ± 4	0.53 ± 0.1	49 ± 5
	Mut	0.43 ± 0.0	33 ± 1[D]	0.23 ± 0.1[C]	26 ± 1[D]
mE7M-129	WT	0.11 ± 0.0	75 ± 1	0.45 ± 0.1	57 ± 7
	Mut	0.20 ± 0.1	77 ± 6	0.14 ± 0.1[C]	45 ± 3
mE7M-B6	WT	0.33 ± 0.2	71 ± 8	0.28 ± 0.2	52 ± 14
	Mut	0.41 ± 0.2	65 ± 7	0.14 ± 0.1	44 ± 2

[^{35}S]GTPγS binding was performed in membranes from whole brains of indicated mouse models as described in Supplemental Methods. [A]EC_{50} and percentage of maximal stimulation values were determined by nonlinear regression analysis (Prism). [B]Results are shown as mean ± SEM of at least 3 independent determinations. [C]$P < 0.05$; [D]$P < 0.01$, compared with WT, 1-way ANOVA with Bonferroni's post hoc test. Mut, homozygous mice.

Table 3. Morphine analgesia

Mouse model	Genotype	Morphine ED_{50} (mg/kg, s.c.)[A]
mE3M-129	WT	2.1 ± 0.4[B]
	Mut	3.3 ± 0.2[C]
mE3M-B6	WT	2.3 ± 0.2
	Mut	3.4 ± 0.2[C]
mE4M-129	WT	2.7 ± 0.1
	Mut	3.2 ± 0.3
mE4M-B6	WT	2.4 ± 0.4
	Mut	3.2 ± 0.5
mE7M-129	WT	2.2 ± 0.3
	Mut	2.8 ± 0.2
mE7M-B6	WT	2.9 ± 0.3
	Mut	2.6 ± 0.5

[A]ED_{50} values from cumulative dose-response curves performed using a radiant-heat tail-flick assay as described in Methods were determined by nonlinear regression analysis (Prism). [B]Results are shown as mean ± SEM of the ED_{50} values determined from at least 3 independent dose-response studies. [C]$P < 0.05$, compared with WT, 1-way ANOVA with Bonferroni's post hoc test. n = 6–14 mice in each dose-response study. Mut, homozygous mice.

(Figure 1C). These results mimic those in mE7M-B6 homozygous mice (Figure 1A), supporting the involvement of exon 7–associated variants in morphine tolerance.

Effect of the C-terminal truncation on morphine physical dependence. Morphine physical dependence was assessed with naloxone-precipitated withdrawal following 5 days of chronic morphine treatment by measuring naloxone-precipitated jumping, a measure of physical dependence (31). Naloxone precipitated significantly less jumping in both mE3M-B6 and mE4M-B6 homozygous mice than their WT B6 control mice (Figure 2A), suggesting a diminished level of dependence. There was no difference in the jumping frequency between the mE7M-B6 WT and homozygous mice. Similarly, no significant change in naloxone-precipitated jumping was seen in CD-1 mice treated with the ANT-vMO targeting intron/exon 7 junction (Supplemental Figure 3). These results suggest that unlike tolerance, morphine dependence is not influenced by exon 7–associated variants in B6 or CD-1 mice.

The WT 129 control mice all showed lower levels of jumping than WT B6 control mice (Figure 2A), consistent with previous observations (31). However, we observed even fewer jumps in E3M-B6 129 homozygous mice. As in the B6 background, the exon 7 truncation in the 129 mice failed to alter jumping, illustrating the differences between these truncation models.

Effect of the C-terminal truncation on morphine conditioned place preference. We investigated the effect of the C-terminal truncation on morphine reward using a conditioned place preference (CPP) paradigm. The strong preferences for the morphine-paired compartment in mE3M-B6 and mE4M-B6 homozygous mice were similar to those seen in their respective WT controls (Figure 2B). In contrast, the mE7M-B6 homozygous mice exhibited significantly lower preference for the drug-paired compartment than the mE7M WT control mice (Figure 2B), suggesting that exon 7–associated variants are involved in morphine reward behavior in B6 mice. Morphine CPP in WT and homozygous 129 mice at the same dose was not robust and was not significant (Supplemental Figure 4), consistent with previous findings (36).

Effect of the C-terminal truncation on morphine locomotor activity. In WT B6 and 129 mice, morphine significantly increased locomotion, with a greater effect in B6 compared with 129 mice (Figure 3A and Supplemental Figure 5), consistent with the literature (37). Both mE4M-B6 and mE7M-B6 homozygous mice showed a modest, but significant, decrease in morphine-induced locomotion measured as total distance traveled compared with their respective WT B6 control mice, while the locomotor activity in mE3M-B6 homozygous mice was not significantly changed (Figure 3A and Supplemental Figure 5). A similar pattern was observed in all the mouse models on the 129 background, but the differences were not significant (Figure 3A). When analyzed by distance per minute, locomotor activity was significantly lower in mE4M-129 homozygous mice than in WT control mice (Supplemental Figure 5). These results indicate a modest effect of the C-terminal truncations in morphine-induced locomotor activity.

Effect of the C-terminal truncation on morphine inhibition of gastrointestinal transit. Morphine modulates gastrointestinal (GI) transit through activation of receptors on the myenteric plexus and centrally (38). Morphine (5 mg/kg) decreased charcoal transit in both B6 and 129 WT mice (Supplemental Figure 6). All the C-terminal truncations had little effect, except for a small, but significant, decrease in morphine's inhibition of GI transit in mE4M-B6 homozygous mice compared with the WT controls (Supplemental Figure 6), consistent with our early observation that an antisense oligo targeting exon 4 reduced morphine inhibition of GI transit (39).

Effect of the C-terminal truncation on morphine-induced catalepsy. High doses of morphine induce catalepsy (40, 41), a condition of diminished responsiveness characterized by a trance-like state and immobility. In B6 mice, morphine produced dose-dependent and time-dependent cataleptic responses (Supplemental Figure 7). We therefore examined morphine catalepsy 30 minutes after mor-

Table 4. Morphine dose-response study before and after chronic morphine treatment

Mouse model	Genotype	Morphine ED_{50} (mg/kg, s.c.)[A]		ED_{50} shift
		Day 1	Day 5	
mE3M-129	WT	2.2 (2.0–2.5)	2.5 (2.2–2.9)	1.2
	Mut	3.1 (2.6–3.7)	8.4 (7.0–10.6)[B,C]	2.7
mE4M-129	WT	2.7 (2.0–3.5)	3.3 (2.4–4.3)	1.2
	Mut	3.4 (2.9–3.8)	8.1 (6.1–10.7)[B,C]	2.4
mE7M-B6	WT	2.8 (2.3–3.5)	14.6 (11.1–19.3)[B]	5.2
	Mut	3.1 (2.6–3.6)	6.9 (6.1–7.8)[B,C]	2.2

[A]ED_{50} values with 95% CIs (parentheses) were determined by nonlinear regression analysis (Prism). ED_{50} values with nonoverlapping 95% CIs were considered significantly different (30). [B]$P < 0.05$, compared with day 1; [C]$P < 0.05$, compared with WT day 5. The number of mice used was as follows: mE3M-129, 8 WT and 7 Mut; mE4M-129, 5 WT and 9 Mut; mE7M-B6, 10 WT and 9 Mut. Mut, homozygous mice.

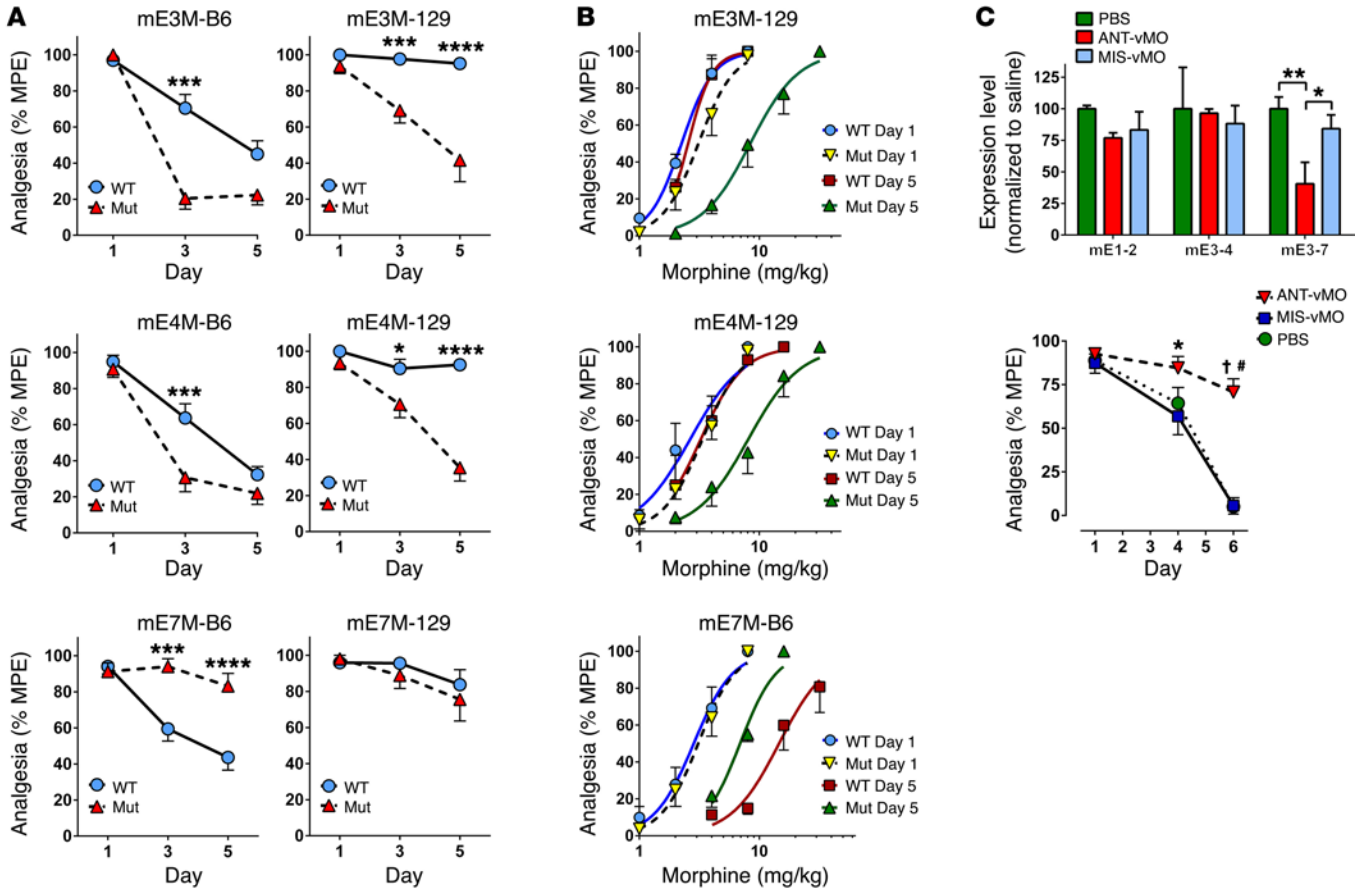

Figure 1. Effect of the C-terminal truncation on morphine tolerance. (**A**) Morphine tolerance in the mutant mice. Tolerance was induced and assessed as described in Methods. The number of mice used were as follows: mE3M-B6, 15 WT and 14 homozygous (Mut) in 2 independent experiments; mE4M-B6, 18 WT and 17 Mut in 2 independent experiments; mE7M-B6, 20 WT and 19 Mut in 3 independent experiments; mE3M-129,15 WT and 11 Mut in 2 independent experiments; mE4M-129, 13 WT and 13 Mut in 2 independent experiments; mE7M-129, 7 WT and 7 Mut in 1 experiment. $^{*}P < 0.05$; $^{***}P < 0.001$; $^{****}P < 0.0001$, 2-way ANOVA with Bonferroni's post hoc test. Mut, homozygous mice. (**B**) Morphine dose-response curve in the mutant mice. Cumulative dose-response studies were performed before (day 1) and after (day 5) morphine treatment (ED_{50} values and number of mice in Table 4). (**C**) ANT-vMO (ANT-vMO targeting intron/exon 7) study in CD-1 mice. Top: mRNA expression of *Oprm1* transcripts containing exons 1–2 (mE1-2), exons 3–4 (mE3-4), and exons 3–7 (mE3-7). RNAs from the PAG dissected on day 6 (see bottom panel) were used in RT-qPCRs. All $2^{-(\Delta Ct)}$ values are normalized with PBS group. Results are shown as the mean ± SEM of at least 3 individual samples. $^{*}P < 0.05$; $^{**}P < 0.01$, 1-way ANOVA with Bonferroni's post hoc test. Bottom: morphine tolerance. Group of mice were i.c.v. injected with 10 μg of ANT-vMO ($n = 18$) or MIS-vMO ($n = 16$), or PBS ($n = 19$), for 4 days (days 1–4). Tolerance was induced by twice-daily morphine injection (10 mg/kg, s.c.) for 5 days (days 2–6). Morphine analgesia was tested on days 1, 4, and 6. Results are from 2 independent experiments. $^{\#}P < 0.0001$, compared with PBS; $^{\dagger}P < 0.0001$, compared with MIS-vMO; $^{*}P < 0.05$, compared with MIS-vMO, 2-way ANOVA with Bonferroni's post hoc test.

phine administration (60 mg/kg, s.c.) in mE3M-B6, mE4M-B6, and mE7M mice. Morphine induced catalepsy in all WT control and homozygous mice when compared with saline controls (Figure 3B). However, the truncated mutant B6 mice showed lower responses than their corresponding WT controls, suggesting involvement of all the C-terminal tails in morphine-induced catalepsy. The effect of truncation on catalepsy was not as robust in 129 mice as in B6 animals. As with the B6 mice, all the WT 129 control mice were cataleptic following morphine, but only mE4M-129 homozygous mice showed a smaller reduction than WT controls (Figure 3B).

Effect of the truncation of exon 7–associated C-terminal tails on [^{35}S]GTPγS binding in brain regions of mice chronically treated with morphine. Receptor desensitization has been proposed as one cellular mechanism contributing to morphine tolerance in both in vitro cell lines and in vivo rodent models (42–45). The reduced morphine tolerance with exon 7 truncation in mE7M-B6 mice raised the question of whether or not the truncation altered receptor desensitization in these mice. We evaluated receptor desensitization by measuring morphine-stimulated [^{35}S]GTPγS binding with membranes from 6 brain regions in the mE7M-B6 models after the 5 days of morphine treatment. There were no significant differences in the EC_{50} values among brain regions or groups of mE7M-B6 mice, and most regions failed to show morphine-induced changes in maximal stimulation in either WT or homozygous mice (Table 5 and Supplemental Figure 8), although the maximal stimulation in the periaqueductal gray (PAG) of saline-treated mE7M-B6 homozygous mice was significantly higher than in WT controls (Table 5 and Supplemental Figure 8). However, morphine treatment reduced the stimulation in the hypothalamus and brain stem in mE7M-B6 WT mice, but not in

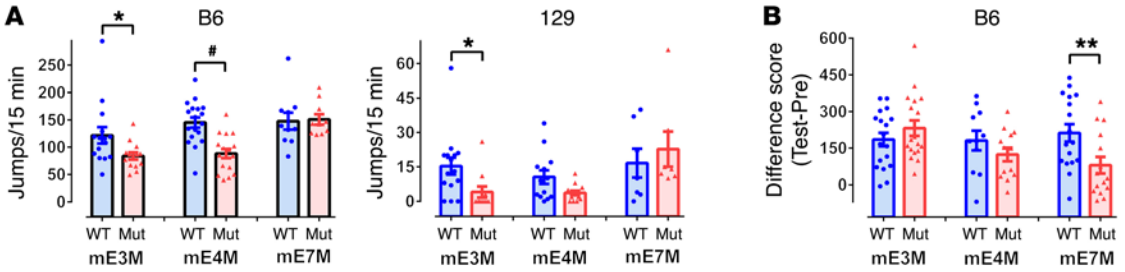

Figure 2. Effect of the C-terminal truncation on morphine physical dependence and CPP in the mutant mice. (**A**) Morphine physical dependence. Morphine physical dependence was assessed by naloxone-precipitated withdrawal after chronic morphine treatment in the mutant mice on B6 or 129 backgrounds, as described in Methods. Results are shown as the number of jumps within 15 minutes immediately following naloxone injection. The number of mice used were as follows: mE3M-B6, 15 WT and 14 Mut in 2 independent experiments; mE4M-B6, 18 WT and 17 Mut in 2 independent experiments; mE7M-B6, 10 WT and 10 Mut in 1 independent experiment; mE3M-129, 15 WT and 11 Mut in 2 independent experiments; mE4M-129, 13 WT and 13 Mut in 2 independent experiments; mE7M-129, 7 WT and 7 Mut in 1 experiment. $^{*}P < 0.05$; $^{\#}P < 0.0001$, compared with WT, 1-way ANOVA with Bonferroni's post hoc test. Mut, homozygous mice. (**B**) Morphine CPP. Morphine CPP was assessed using a 3-chamber apparatus (Med Associates) with a 6-day paradigm as described in Methods. Results were calculated by different scores (seconds) in drug-paired chamber between the test day and preconditioning day and from 2 independent experiments. The number of mice used were as follows: mE3M-B6, 18 WT and 18 Mut; mE4M-B6, 11 WT and 13 Mut; mE7M-B6, 17 WT and 15 Mut. $^{**}P < 0.01$, compared with WT, 1-way ANOVA with Bonferroni's post hoc test.

mE7M-B6 homozygous mice (Figure 4 and Table 5). Binding studies from the same hypothalamus and brain stem tissues revealed no change in [^{3}H]DAMGO binding after morphine treatment or between genotypes (Supplemental Table 4). Thus, these results suggest that morphine treatment desensitized mu opioid receptor coupling with G proteins in the hypothalamus and brain stem in WT mE7M-B6 mice and that this desensitization was lost in truncated mutant mE7M-B6 mice.

mE7M-129 WT mice did not develop tolerance to morphine, so it was not surprising that morphine treatment failed to significantly alter the maximal stimulation in any brain regions (Table 5). However, we observed elevated stimulation levels in saline-treated mE7M-129 homozygous mice compared with their WT controls in both the hypothalamus and brain stem (Table 5). Similar elevation was seen in the PAG of mE7M-B6 homozygous mice (Table 5).

We did not examine the mE3M and mE4M mouse models because the decreased receptor expression and [^{35}S]GTPγS binding in the naive truncate mutant mice (Tables 1 and 2) might have made interpretation difficult.

Effect of the truncation of exon 7–associated C-terminal tails on ERK1/2 activation in brain regions of mice chronically treated with morphine. ERK1/2 activation has been linked to receptor desensitization through arrestin-dependent and/or arrestin-independent mechanisms, which may contribute to morphine tolerance (42, 46). We investigated ERK activation with Western blots from the same 6 brain regions in mE7M-B6 mice after 5 days of morphine or saline treatment. While chronic morphine failed to alter ERK phosphorylation levels in most regions, including the striatum, PAG, hypothalamus, and brain stem in either WT control or homozygous mice (Supplemental Figure 9), it increased ERK1/2 phosphorylation in the thalamus of WT B6 control mice, raising questions regarding the role of ERK activation in the thalamus in morphine tolerance and its relationship with receptor desensitization in the hypothalamus and brain stem. Similarly to WT B6 controls, mE7M-B6 homozygous mice showed increased ERK activation in the thalamus after morphine treatment, with no changes in other regions (Supplemental Figure 9), suggesting it is unlikely that exon 7–associated C-terminal sequences are involved in the ERK1/2 activation.

In vitro characterization of exon 7–associated 7-TM variants. In view of the potential role of exon 7–containing variants in morphine action, we compared the exon 7–associated 7-TM variants mMOR-1C and mMOR-1O with the exon 4–associated mMOR-1 in stably transfected CHO cells. First, we examined signaling bias. Using appropriately engineered stable CHO cell lines, we examined mu agonist–induced β-arrestin recruitment using a PathHunter β-arrestin 2 assay (DiscoverX) and G protein activation by [^{35}S]GTPγS binding. Overall, the mu agonists morphine, endomorphin 1, and fentanyl stimulated [^{35}S]GTPγS binding with full efficacy relative to DAMGO, with the exception of mMOR-1O, in which the maximal stimulation by morphine was significantly reduced (Figure 5A and Supplemental Table 5). We observed marked potency differences among the variants. For example, DAMGO was most potent against mMOR-1, with an EC_{50} of 17 nM, compared with 195 and 157 nM against mMOR-1C and mMOR-1O, respectively. Endomorphin 1 and fentanyl also were far less potent against the exon 7–associated variants. The compounds also stimulated β-arrestin 2 recruitment with varying efficacies relative to DAMGO. Although morphine was the least effective against all 3 variants, it stimulated β-arrestin 2 binding more efficaciously in mMOR-1O than in mMOR-1 and mMOR-1C, with no significant changes in potencies. Endomorphin 1 also had higher E_{max} (maximum response achievable) values against mMOR-1O than mMOR-1, with no difference in their EC_{50} values. Both DAMGO and endomorphin 1 had higher EC_{50} values in mMOR-1C than in mMOR-1 and mMOR-1O.

Using those 2 assays, we calculated the bias factors of the drugs among the variants using the Black and Leff operational model (refs. 47, 48, and Figure 5B). Compared with the bias of DAMGO against mMOR-1, which was normalized to a value of 1, we observed marked variability among the drugs and among the variants, with the greatest difference being a bias factor of –44.3 for fentanyl against mMOR-1O (Figure 5B). When each drug was normalized to mMOR-1 (Figure 5B), they all displayed a great-

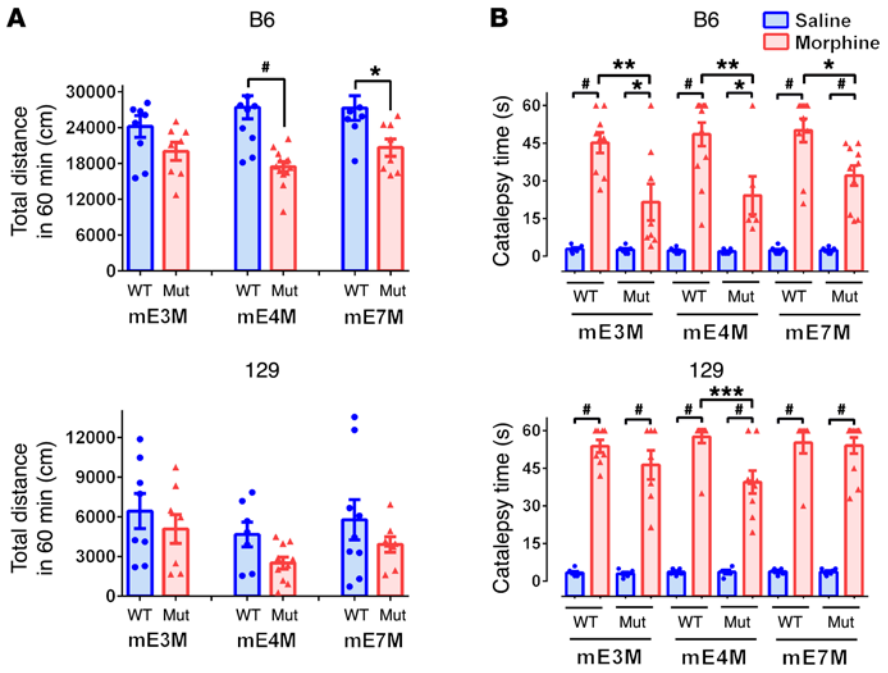

Figure 3. Effect of the C-terminal truncation on morphine locomotor activity and catalepsy in the mutant mice. (**A**) Morphine locomotor activity. Morphine locomotor activity of the mutant mice on B6 and 129 backgrounds was measured in an open-field chamber (Med Associates) as described in Supplemental Methods. Following morphine injection (10 mg/kg, i.p.), the total distance traveled (cm) within 60 minutes was measured. Results are shown as mean ± SEM. The number of mice used were as follows: mE3M-B6, 9 WT and 8 Mut; mE4M-B6, 11 WT and 13 Mut; mE7M-B6, 9 WT and 8 Mut; mE3M-129, 8 WT and 8 Mut; mE4M-129, 7 WT and 10 Mut; mE7M-129, 9 WT and 8 Mut. $^{*}P < 0.01$; $^{\#}P < 0.0001$, compared with WT, 1-way ANOVA with Bonferroni's post hoc test. Mut, homozygous mice. (**B**) Morphine catalepsy. Morphine catalepsy in the mutant mice was assessed by using a horizontal bar test as described in Supplemental Methods. Mice were tested 30 minutes after morphine injection (60 mg/kg, s.c.). The time (s) spent in cataleptic position was recorded. Results are shown as mean ± SEM. The number of mice used were as follows: in mE3M-B6, 6 WT-Saline, 9 WT-morphine, 6 Mut-Saline, 8 Mut-morphine; in mE4M-B6, 6 WT-Saline, 12 WT-morphine, 6 Mut-Saline, 6 Mut-morphine; in mE7M-B6, 8 WT-Saline, 10 WT-morphine, 8 Mut-Saline, 10 Mut-morphine; in mE3M-129, 6 WT-Saline, 8 WT-morphine, 6 Mut-Saline, 7 Mut-morphine; in mE4M-129, 5 WT-Saline, 10 WT-morphine, 5 Mut-Saline, 9 Mut-morphine; in mE7M-129, 5 WT-Saline, 7 WT-morphine, 6 Mut-Saline, 11 Mut-morphine. $^{*}P < 0.05$; $^{\#}P < 0.0001$, compared with group treated with Saline; $^{*}P < 0.05$; $^{**}P < 0.01$; $^{***}P < 0.001$, compared with WT treated with morphine, 2-way ANOVA with Bonferroni's post hoc test.

er β-arrestin 2 bias with the exon 7–associated variants. Of the 2 exon 7–associated variants, mMOR-1O showed greater β-arrestin 2 bias than mMOR-1C. For example, relative to mMOR-1, the bias factor for mMOR-1C was approximately 4-fold lower (–2.2) than for mMOR-1O (–10.0) in response to fentanyl. Structurally, both variants have exon 7, but mMOR-1C is extended for an additional 22 aa encoded by exons 8 and 9 beyond the 30 aa encoded by exon 7. This extended sequence is likely responsible for the diminished bias relative to exon 7 coding sequences alone. When the drugs were normalized to DAMGO within each variant, they all showed similar β-arrestin 2 bias patterns (Figure 5B).

We then examined DAMGO- and morphine-induced receptor desensitization in a [^{35}S]GTPγS-binding assay in CHO cells stably transfected with either mMOR-1, mMOR-1C, or mMOR-1O, as previously described (25, 49). Although both DAMGO and morphine induced rapid desensitization in all variants, the desensitization was slightly more rapid in the mMOR-1O cells (Supplemental Figure 10A).

Finally, we compared the sodium sensitivity of [^{3}H]DAMGO binding in the 3 CHO cell lines. Sodium acts allosterically to stabilize receptors in an antagonist conformation, which has lower affinity for agonist binding (50–52). Sodium ions lowered [^{3}H]DAMGO binding in a dose-dependent manner for all 3 receptors (Supplemental Figure 10B). However, mMOR-1O stood apart from the other 2, displaying a decreased sensitivity to the ion. This was quite interesting in that the sodium site is located within the transmembrane region of the receptor (51), which is common to all 3 variants. These studies revealed a general pattern in vitro of differences between exon 7–associated and exon 4–associated 7–TM C-terminal variants.

Discussion

The current study used 3 mutant mouse models, mE3M, mE4M, and mE7M, on 2 inbred strain backgrounds to investigate the importance of *Oprm1* 3′ splicing and the distal C-terminal tails of mu opioid receptors in mediating complex morphine actions (see summary in Table 6). These truncation models did not substantially affect morphine analgesia, but differentially altered morphine-induced tolerance, physical dependence, reward behavior, and locomotor activity profiles. The loss of morphine-induced receptor desensitization in the hypothalamus and brain stem of mE7M-B6 mutant mice further implicated the involvement of exon 7–associated variants in morphine-induced receptor desensitization and tolerance. The similarity in several morphine-induced behaviors and receptor desensitization between mE7M-B6 homozygous and β-arrestin 2 KO mice suggests a physical and functional association of exon 7–associated C-terminal tails with β-arrestin 2, a hypothesis further supported by our in vitro data showing that several mu agonists displayed greater β-arrestin bias against exon 7–associated variants than against the exon 4–associated mMOR-1.

Loss of the exon 4 epitope reduced both [^{3}H]naloxone receptor binding and maximal mu agonist–stimulated [^{35}S]GTPγS binding levels despite the lack of significant changes in mRNA levels. The 12 amino acids encoded by exon 4 contain a MOR-1–derived recycling sequence (MRS) that facilitates recycling of internalized MOR-1 to the plasma membrane following DAMGO treatment in HEK293 cells (29). Loss of the MRS enhanced agonist-induced receptor trafficking to lysosomes for degradation. The loss of the MRS in both mE3M and mE4M homozygous mice corresponds with our observed decreases in receptor sites and [^{35}S]GTPγS stimulation and raises an interesting question of whether the MRS has a similar role under endogenous opioid tone in vivo.

Table 5. Morphine-stimulated [^{35}S]GTPγS binding in membranes from brain regions

Region	Mouse	mE7M-B6		mE7M-129	
		% Maximum stimulation[A]	EC_{50} (μM)[A]	% Maximum stimulation	EC_{50} (μM)
Striatum	WT-Saline	38 ± 2	0.3 ± 0.0	41 ± 3	0.4 ± 0.1
	WT-morphine	30 ± 5	0.4 ± 0.1	39 ± 3	0.4 ± 0.1
	Mut-Saline	49 ± 4[B]	0.3 ± 0.1	41 ± 2	0.6 ± 0.2
	Mut-morphine	37 ± 3	0.3 ± 0.0	43 ± 2	0.6 ± 0.3
Nucleus accumbens	WT-Saline	77 ± 2	0.5 ± 0.0	95 ± 5	0.3 ± 0.1
	WT-morphine	77 ± 5	0.7 ± 0.2	95 ± 11	0.3 ± 0.0
	Mut-Saline	73 ± 7	0.9 ± 0.3	95 ± 16	0.3 ± 0.1
	Mut-morphine	83 ± 10	0.5 ± 0.2	86 ± 6	0.2 ± 0.1
Thalamus	WT-Saline	61 ± 5	0.2 ± 0.1	66 ± 8	0.2 ± 0.0
	WT-morphine	49 ± 2	0.3 ± 0.1	76 ± 5	0.3 ± 0.1
	Mut-Saline	53 ± 3	0.2 ± 0.1	76 ± 9	0.3 ± 0.1
	Mut-morphine	57 ± 7	0.2 ± 0.1	79 ± 3	0.2 ± 0.0
Hypothalamus	WT-Saline	61 ± 2[B]	0.3 ± 0.0	86 ± 8	0.2 ± 0.0
	WT-morphine	43 ± 5	0.2 ± 0.0	104 ± 13	0.2 ± 0.0
	Mut-Saline	62 ± 3[B]	0.2 ± 0.0	106 ± 13[C]	0.2 ± 0.1
	Mut-morphine	72 ± 1[D]	0.2 ± 0.0	96 ± 8	0.2 ± 0.1
PAG	WT-Saline	42 ± 3	0.5 ± 0.2	31 ± 4	0.3 ± 0.0
	WT-morphine	49 ± 3	0.5 ± 0.1	33 ± 8	0.2 ± 0.0
	Mut-Saline	59 ± 4[C]	0.3 ± 0.1	33 ± 7	0.2 ± 0.1
	Mut-morphine	54 ± 1	0.4 ± 0.2	24 ± 4	0.6 ± 0.2[B,C,E]
Brainstem	WT-Saline	50 ± 3[B]	0.4 ± 0.2	45 ± 2	0.1 ± 0.0
	WT-morphine	31 ± 7	0.3 ± 0.1	62 ± 2	0.1 ± 0.0
	Mut-Saline	50 ± 6[B]	0.3 ± 0.1	71 ± 7[C]	0.3 ± 0.1
	Mut-morphine	48 ± 1[F]	0.3 ± 0.1	71 ± 7[C]	0.2 ± 0.0

Morphine (M) tolerance was induced in mE7M-B6 and mE7M-129 mouse models by the same paradigms used in Figure 1. A control group injected with saline (S) was also included for both WT and homozygous mice. [^{35}S]GTPγS-binding assay was performed using membranes prepared from 6 regions that were dissected after the last morphine injection on day 5, as described in Supplemental Methods. Percentage of maximal stimulation (over basal level) and EC_{50} values were calculated by nonlinear regression analysis (Prism). [A]Results are shown as mean ± SEM of the EC_{50} and percentage of maximal stimulation values determined from 3 to 4 independent experiments. Two-way ANOVA with Bonferroni's post hoc test was used. [B]$P < 0.01$, compared with WT treated with morphine. [C]$P < 0.05$, compared with WT treated with Saline. [D]$P < 0.0001$, compared with WT treated with morphine. [E]$P < 0.01$, compared with homozygous treated with Saline. [F]$P < 0.05$, compared with WT treated with morphine. Morphine-stimulated dose-response curves are shown in Supplemental Figure 8. Mut, homozygous mice.

Distal C-terminal sequences markedly affected morphine tolerance, with opposite effects seen between exon 4– and exon 7–associated C-terminal truncation models. This was particularly interesting in view of the lack of change in morphine analgesia among the truncation models, despite receptor binding decreases of 30% to 50% in mE4M and mE3M models. Maintaining analgesic activity with reduced receptor expression has been reported previously in mu receptor KO models in which loss of half the receptor in the heterozygotes failed to change morphine's analgesic ED_{50} values (33, 34). Removal of the exon 4–encoded 12 aa in mMOR-1, the predominant 7TM variant, facilitated morphine tolerance in mE4M homozygous mice on both B6 and 129 backgrounds, implying that expression of the exon 4–encoded sequence impedes the development of morphine tolerance. It is interesting to consider whether the loss of the MRS sequence and its ability to recycle mMOR-1 contributes to this enhanced sensitivity to the production of tolerance. This possibility is further supported by a mutant DMOR mouse model in which a portion of exon 3–encoded sequences in mMOR-1 was replaced by a portion of the C terminus of the δ opioid receptor mDOR-1 with the elimination of all the C-terminal downstream from exon 3, similarly to our mE3M mice (53). As with our mice, the DMOR animals developed tolerance to morphine more rapidly than WT controls.

The role of the exon 7–associated C-terminal truncation in morphine tolerance was opposite that of the exon 4–encoded C-terminal truncation. Loss of the exon 7 sequence attenuated morphine tolerance in the mutated animals. Furthermore, this association of the exon 7–associated variants with morphine tolerance was further supported by the reduction of morphine tolerance by the downregulation of exon 7–associated variants by an ANT-vMO. Thus, the exon 7–associated and exon 4–encoded C-terminal tails appear to have opposing functions, with the exon 7–associated tails facilitating tolerance and the exon 4–encoded tails diminishing it.

Receptor desensitization in specific brain regions, including brain stem nuclei, has been previously observed autoradiographically using DAMGO-stimulated [^{35}S]GTPγS in chronic morphine tolerance mouse and rat models (54, 55), with similar results in membrane-binding studies from morphine-tolerant mouse brain stem (56). In our study, morphine-tolerant control WT mE7M-B6 mice exhibited reduced morphine-stimulated G protein coupling in the brain stem following chronic morphine treatment, consistent with previous observations. Our study also revealed receptor desensitization in the hypothalamus. Mu opioid receptor agonist–induced desensitization involves many proteins in various cellular processes, such as receptor phosphorylation, β-arrestin 2 binding, and internalization (42). These studies raised questions regarding regional expression and function of these proteins as well as regional processing of these cellular events. The prevention of receptor desensitization in both the brain stem and hypothalamus by the exon 7–associated C-terminal truncation in B6 mice suggests a contribution of the exon 7–associated C-terminal variants to morphine-induced receptor desensitization and tolerance. Also, the WT control mE7M-129 mice failed to show the

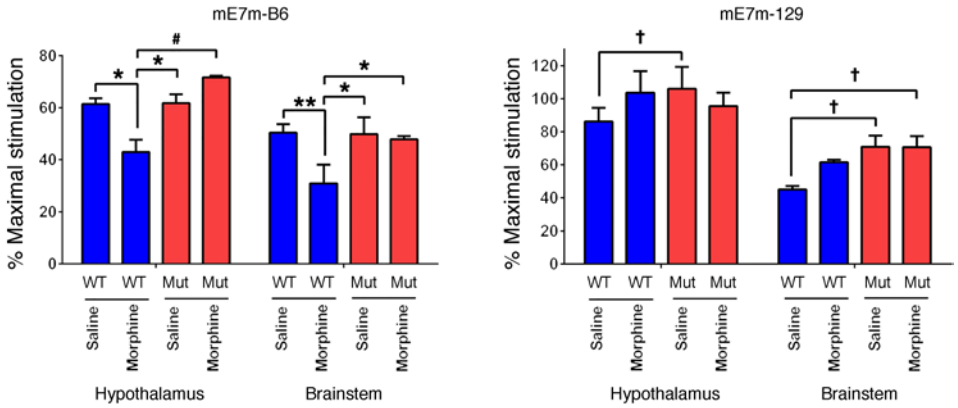

Figure 4. Effect of the truncation of exon 7–encoded C-terminal tails on morphine-induced receptor desensitization by morphine-stimulated [^{35}S]GTPγS binding in the hypothalamus and brain stem. Morphine tolerance was induced in mE7M-B6 and mE7M-129 mouse models by the same paradigms used for Figure 1. A control group injected with saline was also included for both WT and homozygous mice. [^{35}S]GTPγS-binding assay was performed using membranes prepared from 6 regions that were dissected after the last morphine injection on day 5, as described in Supplemental Methods. Percentage of maximal stimulation (over basal level) and EC_{50} values were calculated by nonlinear regression analysis (Prism). Only percentage of maximal stimulation in the hypothalamus and brain stem in mE7M-B6 and mE7M-129 mice are shown. The EC_{50} and percentage of maximal stimulation of all the regions among WT and homozygous mice treated with saline or morphine are listed in Table 5 and dose-response curves in Supplemental Figure 8. The results are shown as mean ± SEM of percentage of maximal stimulation values determined from 3 to 4 independent experiments. $^{*}P < 0.05$; $^{**}P < 0.01$; $^{\#}P < 0.001$, compared with WT treated with morphine. $^{\dagger}P < 0.05$, compared with WT treated with saline, 2-way ANOVA with Bonferroni's post hoc test. Mut, homozygous mice.

receptor desensitization in any of the brain regions, including the brain stem and hypothalamus, consistent with the lack of tolerance in these animals in this tolerance paradigm.

Intriguingly, several morphine-induced responses in a β-arrestin 2 KO mouse were similar to those in a mE7M-B6 homozygous mouse (Table 6), including reduced morphine tolerance (56, 57), loss of the receptor desensitization in the brain stem (56), no alteration of physical dependence (56, 58) and GI transit inhibition in the small intestine (59), and reduced locomotor activity (60). However, β-arrestin 2 KO mice also showed some differences from mE7M-B6 homozygous mice, such as enhanced morphine analgesia (61) and CPP (ref. 60 and Table 6). Nevertheless, these similar responses in both models are consistent with a physical and functional interaction of the exon 7–associated C-terminal tails with β-arrestin 2 in producing morphine-induced receptor desensitization in specific regions and morphine tolerance. Our in vitro observations of greater β-arrestin 2 bias with exon 7–associated variants, particularly mMOR-1O, further support this possibility.

Mu agonist–induced receptor phosphorylation and subsequent β-arrestin binding have been postulated as one mechanism of receptor desensitization and mu opioid tolerance (42–44). For example, serine 375 (S375) of MOR-1 in exon 3–encoded C-terminal sequences shared by all C-terminal variants can be phosphorylated mainly by GRK5 (62), contributing to β-arrestin recruitment (63). A S375A mutant mouse displayed reduced tolerance to fentanyl, but not to morphine (64). Phosphorylation of threonine 394 (T394) in the exon 4–encoded C-terminal sequence was involved in mu agonist–induced receptor internalization and desensitization (65, 66). A T394A mutant mouse showed attenuated acute morphine tolerance and increased heroin-taking behavior (67). A number of phosphorylation sites for various protein kinases, such as GPCR kinases (GRKs), are predicted in exon 7–associated C-terminal tails (Supplemental Figure 11 and ref. 68), raising the possibility of enhanced phosphorylation and increased β-arrestin recruitment in these variants. The exon 7–encoded C-terminal sequences also contain a consensus β-arrestin 2 binding motif, PxPxxE or PxxPxxE (Supplemental Figure 11), that interacts with positively charged residues at the N terminus of β-arrestin 2, based on homology modeling with the recent crystal structure of the rhodopsin-arrestin complex as a template (ref. 69 and H. Eric Xu, personal communication). Although only a prediction, it will be interesting to see how this motif influences β-arrestin 2 binding and receptor signaling as well as morphine actions in vivo.

The exon 7 truncation also selectively and markedly reduced morphine CPP in the B6 mice, while the other 2 truncation models did not. Conversely, the exon 7–associated C-terminal tails did not affect naloxone-precipitated jumping in B6 mice, while the other 2 B6 truncation models did. However, some behaviors were similarly altered by the truncations, such as the lowered locomotor activity in B6 mice. Together, the divergent effects seen in these mutant mice among various morphine actions strongly support the functional significance of 3′ alternative splicing of the *Oprm1* gene and illustrate selective roles for specific C-terminal tails in various actions.

While the models dissociate the actions of different groups of C-terminal splice variants, assigning a specific variant is not possible due to concurrent 5′ alternative splicing, which yields multiple variants with identical C-terminal sequences (Supplemental Figure 1 and Supplemental Figure 2B). For example, the exon 4 epitope is contained within a number of 7TM variants (mMOR-1, mMOR-1H, mMOR-1i, and mMOR-1J) as well as a 6TM variant (mMOR-1G). The exon 7–encoded sequence is present in 7TM variants (mMOR-1C, mMOR-1O, and mMOR-1U) as well as the 6TM variant mMOR-1M. While the far greater affinity of morphine for 7TM receptors in binding assay and the retention of morphine analgesia in an E11-KO mouse lacking 6TM variants (34, 70–73) implies that morphine is more likely to interact with 7TM receptors, our recent studies revealed a decrease in mor-

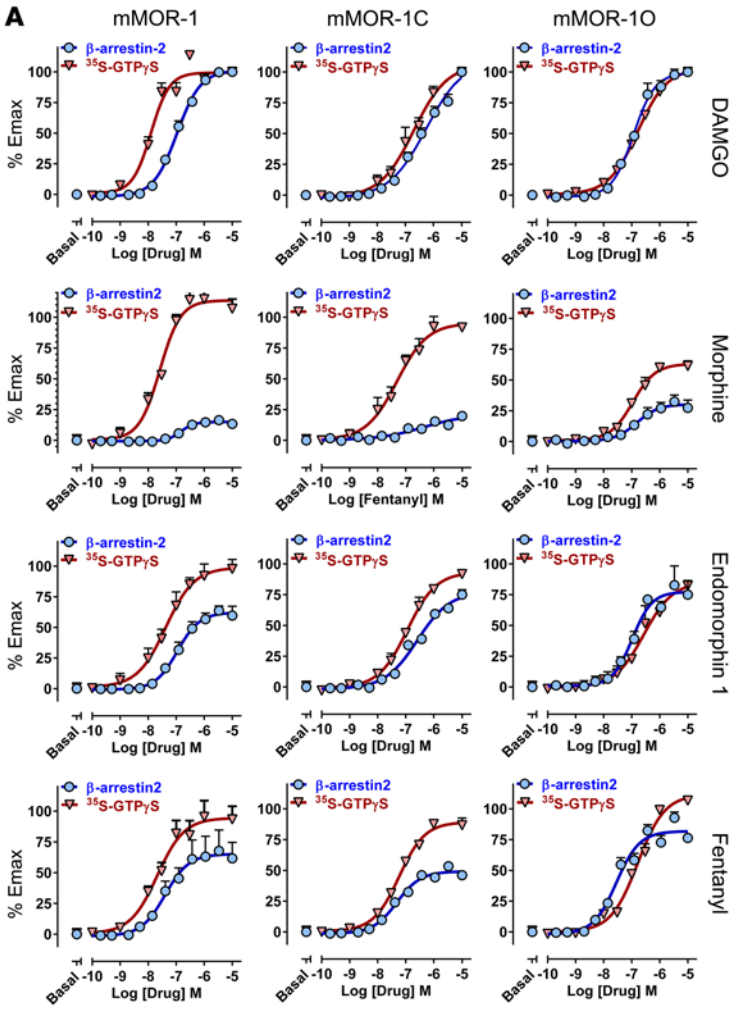

B

Normalized to DAMGO at mMOR-1

	mMOR-1	mMOR-1C	mMOR-1O
DAMGO	1.0	-1.9	-10.2
Morphine	-1.5	-1.3	-5.0
Endomorphin 1	-3.3	-4.8	-19.4
Fentanyl	-4.4	-9.8	-44.3

Normalized to drug at mMOR-1

	mMOR-1	mMOR-1C	mMOR-1O
DAMGO	1.0	-1.9	-10.2
Morphine	1.0	1.2	-3.3
Endomorphin 1	1.0	-1.5	-6.0
Fentanyl	1.0	-2.2	-10.0

Normalized to DAMGO at each variant

	mMOR-1	mMOR-1C	mMOR-1O
DAMGO	1.0	1.0	1.0
Morphine	-1.5	1.5	2.1
Endomorphin 1	-3.3	-2.4	-1.9
Fentanyl	-4.4	-5.0	-4.3

Figure 5. Mu opioid receptor agonist–induced β-arrestin 2 recruitment and G protein activation in CHO cells stably transfected with exon 4–associated mMOR-1 and exon 7–associated mMOR-1C and mMOR-1O. (**A**) β-arrestin 2 recruitment and G protein activation. A PathHunter β-arrestin 2 assay (DiscoverX) and [^{35}S]GTPγS-binding assay were performed in an engineered CHO cell line stably transfected with mMOR-1, mMOR-1C, or mMOR-1O, as described in Methods. Each dose-response curve is from 3 independent experiments and normalized to maximal DAMGO stimulation (10 μM DAMGO) at the particular receptor variant for comparison across drugs. The E_{max} and EC_{50} values are listed in Supplemental Table 5. (**B**) Heat map of biased factors. Biased factors were calculated using the Black and Leff operational model (47, 48) by using 2 different normalization methods, 1 normalized with respect to DAMGO at mMOR-1 for a comparison across variants or drugs, and the other, with respect to every individual drug at mMOR-1 for a comparison across variants.

phine tolerance in the E11-KO mouse (our unpublished observations), raising the interesting possibility of a role of the 6TM variant mMOR-1M.

The involvement of exon 7–associated variants in morphine tolerance, reward, and locomotor activity raises the possibility that selectively targeting them may provide potential therapeutic advantages, as shown by our ANT-vMO study. This oligo markedly reduced exon 3/exon 7 splicing and expression of exon 7–associated variants and attenuated morphine tolerance without affecting morphine dependence, mimicking the effect of truncation of exon 7–associated C-terminal tails in mE7M-B6 homozygous mice. Antisense morpholino oligos have been successfully used to correct aberrant splicing in a growing number of animal models of human diseases, such as spinal muscular atrophy (74–76), Duchenne muscular dystrophy (77, 78), and β-thalassemia (79, 80). Our results provide another example where an in vivo antisense morpholino approach might be of clinical value one day.

C-terminal splice variants are not limited to the *OPRM1* gene. Genomic database analysis suggests that as many as 12% of human GPCR genes (excluding olfactory receptor genes) generate alternatively spliced intracellular C-terminal tail variants (our unpublished observation). However, the expression and function of the majority of these C-terminal variants remain unknown. Our studies suggest that the different C termini generated from 3′ alternative splicing of the mu opioid receptor gene are pharmacologically relevant, raising the more general question of whether 3′ alternative splicing may expand the pharmacological repertoire of GPCRs in general.

Methods

Detailed experimental procedures for generation of gene-targeted mutant mice, RT-qPCR, opioid receptor binding, [^{35}S]GTPγS binding, receptor desensitization study, Western blot, locomotor activity, GI motility assay, and catalepsy are described in the Supplemental Methods.

Table 6. Comparison of behavioral and biochemical studies in targeted mice

	Targeted mouse model[A]						
	mE3M Truncation of all C termini		mE4M Truncation of exon 4–encoded C termini		mE7M Truncation of exon 7–encoded C termini		β-arrestin 2 KO[B]
Strain/morphine	129	B6	129	B6	129	B6	B6/129svJ
Analgesia	No change	No change	No change	No change	No change	No change	Enhanced (61)[C]
Locomotor activity	No change	No change	No change	Reduced	No change	Reduced	Reduced (60)[D]
Tolerance	Developed	Enhanced	Developed	Enhanced	No change	Reduced	Reduced (56, 57)[D]
Physical dependence	Reduced	Reduced	No change	Reduced	No change	No change	No change (56, 58)[D,E]
Reward (CPP)	No change	No change	No change	No change	No change	Reduced	Enhanced (60)[C]
Inhibition of GI transit	No change	No change	No change	Reduced	No change	No change	No change (59)[D]
Catalepsy	No change	Reduced	Reduced	Reduced	No change	Reduced	
Receptor desensitization in hypothalamus[F]					No change	Lost	
Receptor desensitization in brain stem[F]					No change	Lost	Lost (56)[D]

[A]All changes are compared with respective WT controls. [B]Data from β-arrestin 2 KO mouse model were from indicated literature. [C]Similar results seen in mE7M-B6 homozygous mice. [D]Divergent results from mE7M-B6 homozygous mice. [E]The physical dependence data in ref. 56 were determined using morphine pellets. There was no change in the physical dependence in β-arrestin 2 KO mice. In ref. 58, when administered using osmotic pump, 2 of 3 doses (12 and 48 mg/kg/d) of morphine did not induce significant reduction of naloxone-precipitated withdrawal (jumps and global score), but 1 dose (24 mg/kg/d) did, in β-arrestin 2 KO mice. [F]Morphine-induced receptor desensitization was assessed by morphine-stimulated (mE7M-B6) (Figure 4) or DAMGO-stimulated (β-arrestin 2 KO) [^{35}S]GTPγS binding (56).

Animals. B6 (stock 000664) and B6 albino (stock 000058) mice were obtained from Jackson Laboratory, 129 mice from Taconic Biosciences, and CD-1 mice from Charles River Laboratories. Adult (8 to 16 weeks old) male mice were used in all experiments. All mice were housed in groups of 5, maintained on a 12-hour light/12-hour dark cycle, and given ad libitum access to food and water.

Generation of gene-targeting mutant mice. Although a traditional KO approach that deletes each individual exon can be used, it may alter the splicing pattern or induce compensatory effects, making the interpretation of phenotypes more difficult. To avoid such a problem, we used a strategy that eliminates the C-terminal tails at the translational level by introducing a stop codon at the end of *Oprm1* exon 3 (mE3M) or the beginning of exon 4 (mE4M) or exon 7 (mE7M) without deletion of any individual exon (see details in Supplemental Methods and Supplemental Table 6).

Morphine analgesia. Analgesia was determined 30 minutes after s.c. injection using a radiant-heat tail-flick assay, with a maximal latency of 10 seconds to minimize tissue damage, as previously described (21, 70). Results were calculated as the percentage of maximum possible effect (% MPE) as follows: [(latency after drug – baseline latency)/(10 – baseline latency) × 100]. Morphine doses used in cumulative dose-response studies were 1, 2, 4, 8, 16, or 32 mg/kg. ED_{50} values were determined using nonlinear regression analysis (GraphPad Prism 6).

Morphine tolerance and physical dependence studies. Tolerance in the targeted mice on a B6 background and CD-1 mice was induced by twice-daily injections with morphine (10 mg/kg, s.c.) for 5 days. Tolerance in the targeted mice on a 129 background was induced by twice-daily injections with escalating doses of morphine (s.c., day 1, 10 mg/kg; days 2 and 3, 20 mg/kg; days 4 and 5, 40 mg/kg). Morphine analgesia was examined on days 1, 3, and 5. Morphine dependence was determined on day 5 with naloxone (s.c., 1 mg/kg for mice on a B6 background and 30 mg/kg for mice on 129 backgrounds and CD-1 mice) injection 3 hours after the last morphine treatment to precipitate withdrawal. The number of jumps within 15 minutes immediately following the naloxone injection was used for the measurement of withdrawal.

In vivo vivo–morpholino oligo study. Morpholino oligos bind to RNA and sterically block access of splicing factors without triggering RNAse H-mediated mRNA degradation, providing advantages in specificity, stability, and low toxicity. The vivo–morpholino oligo is a modified morpholino oligo covalently linked with an octa-guanidine dendrimer that greatly improves delivery efficiency in vivo. CD-1 mice were i.c.v. administered daily for 4 days (days 1–4) with 10 μg of an ANT-vMO (5′-AGGGTTGGCTGTACAAGAAAAAGGA-3′, Gene Tools) targeting intron/exon 7 junction and MIS-vMO (5′-GAGTGTGGTCTGACAAAGAAAGAGA-3′) and PBS. Morphine injection (10 mg/kg, s.c. twice daily) was started on the second day of the vivo–morpholino oligo injection for 5 days (days 2–6) to induce tolerance. Morphine analgesia was assessed on days 1, 4, and 6. Morphine dependence was evaluated on day 6 with naloxone (30 mg/kg) as described above.

CPP. CPP was performed using a 3-chamber apparatus (Med Associates) with a 6-day paradigm. On day 1, mice were placed in the central chamber for 1 minute of habituation with the sliding doors closed, followed by a 20-minute preconditioning period of free exploration in the 3 chambers. Time spent in each chamber was recorded. On days 2 to 5, mice were i.p. injected with saline (morning) or morphine (10 mg/kg, afternoon) and confined to either the black or the white chamber for 20 minutes. On day 6, mice were placed for a 1-minute habituation in the central chamber, followed by a 20-minute free exploration in the 3 chambers. Time spent in each chamber was recorded. Preference was defined as difference between the times spent in the morphine-paired side of the chamber on the test day (day 6) compared with the preconditioning day (day 1).

β-Arrestin 2 recruitment assay. β-arrestin 2 recruitment was determined with the PathHunter enzyme complementation assay (DiscoverX) using engineered CHO cells stably transfected with mMOR-1, mMOR-1C, and mMOR-1O constructs in a Prolink vector (DiscoverX). Cells were plated at a density of 2500 cells/well in a 384-well plate as described in the manufacturer's protocol. The following day, cells were treated with the indicated compound with various concentrations in triplicate for 90 minutes at 37°C, followed by incubation with

PathHunter detection reagents for 60 minutes. Chemiluminescence was measured with an Infinite M1000 Pro plate Reader (Tecan).

Statistics. All mice were randomized and assigned to groups. Some, but not all, experiments were performed under blinded conditions. All statistical analysis was carried out using GraphPad Prism 6. A 1-way ANOVA or 2-way ANOVA was performed with post hoc Bonferroni's multiple comparisons test as described in the figure legends. Data represented the mean ± SEM of at least 3 independent experiments. Statistical significance was set at $P < 0.05$.

Study approval. All animal studies were approved by the IACUC of Memorial Sloan Kettering Cancer Center.

Author contributions

LC, AM Rajadhyaksha, GWP, and YXP designed experiments. JX, ZL, VPLR, AN, AH, MX, TGB, WFH, GCR, RCR, A Martínez-Rivera, DLB, and YXP performed experiments. LC, AM Rajadhyaksha, DLB, and YXP contributed new reagents/analytic tools. LX, ZL, VPLR, AN, AH, TGB, WFH, GCR, RCR, A Martínez-Rivera, AM Rajadhyaksha, and YXP analyzed data. JX, ZL, AN, GWP, and YXP wrote the manuscript.

Acknowledgments

This work was supported by the NIH (DA013997 and DA029244 to YXP, DA06241 and DA07242 to GWP, DA029122 to AM Rajadhyaksha, and DA029122S2 to A Martínez-Rivera, and a core grant from the National Cancer Institute to Memorial Sloan Kettering Cancer Center, CA08748). We thank Chingwen Yang (Gene Targeting Resource Center, The Rockefeller University) for providing the DTA plasmid and generating targeted ES cells, Connie Zhao (Genomics Resource Center, The Rockefeller University) for help genotyping SNPs using a Mouse Medium Density Linkage SNP panel (Illumina) in speed congenic breeding, Margaret Leversha (Molecular Cytogenetics Core, Memorial Sloan Kettering Cancer Center) for help karyotyping ES clones, Willie Mark (Mouse Genetics Core, Memorial Sloan Kettering Cancer Center) for help generating targeted mice, and DiscoverX Corporation for assisting β-arrestin 2 recruitment assay.

Address correspondence to: Ying-Xian Pan, Department of Neurology, Memorial Sloan Kettering Cancer Center, 1275 York Ave., New York, New York 10065, USA. Phone: 646.888.2167; E-mail: pany@mskcc.org.

1. Pasternak GW. Pharmacological mechanisms of opioid analgesics. *Clin Neuropharmacol*. 1993;16(1):1–18.
2. Foley KM. Management of Cancer Pain. In: DeVita VT, Hellman S, Rosenberg SA, eds. *Cancer: Principles and Practice of Oncology*. 2nd ed. New York, New York, USA: Lippincott; 1985:1940–1961.
3. Payne R, Pasternak GW. Pain. In: Johnston MV, Macdonald RL, Young AB, eds. *Principles Of Drug Therapy In Neurology*. Vol. 37. Philadelphia, Pennsylvania, USA: F.A. Davis; 1992:268–301.
4. Ling GS, MacLeod JM, Lee S, Lockhart SH, Pasternak GW. Separation of morphine analgesia from physical dependence. *Science*. 1984;226(4673):462–464.
5. Moulin DE, Ling GS, Pasternak GW. Unidirectional analgesic cross-tolerance between morphine and levorphanol in the rat. *Pain*. 1988;33(2):233–239.
6. Chang A, Emmel DW, Rossi GC, Pasternak GW. Methadone analgesia in morphine-insensitive CXBK mice. *Eur J Pharmacol*. 1998;351(2):189–191.
7. Wolozin BL, Pasternak GW. Classification of multiple morphine and enkephalin binding sites in the central nervous system. *Proc Natl Acad Sci U S A*. 1981;78(10):6181–6185.
8. Pan YX. Diversity and complexity of the mu opioid receptor gene: alternative pre-mRNA splicing and promoters. *DNA Cell Biol*. 2005;24(11):736–750.
9. Pasternak GW, Pan YX. Mu opioids and their receptors: evolution of a concept. *Pharmacol Rev*. 2013;65(4):1257–1317.
10. Markovic D, Challiss RA. Alternative splicing of G protein-coupled receptors: physiology and pathophysiology. *Cell Mol Life Sci*. 2009;66(20):3337–3352.
11. Wise H. The roles played by highly truncated splice variants of G protein-coupled receptors. *J Mol Signal*. 2012;7(1):13.
12. Oladosu FA, Maixner W, Nackley AG. Alternative splicing of G protein-coupled receptors: relevance to pain management. *Mayo Clin Proc*. 2015;90(8):1135–1151.
13. Pan YX, Xu J, Mahurter L, Bolan E, Xu M, Pasternak GW. Generation of the mu opioid receptor (MOR-1) protein by three new splice variants of the Oprm gene. *Proc Natl Acad Sci U S A*. 2001;98(24):14084–14089.
14. Pan YX, Xu J, Xu M, Rossi GC, Matulonis JE, Pasternak GW. Involvement of exon 11-associated variants of the mu opioid receptor MOR-1 in heroin, but not morphine, actions. *Proc Natl Acad Sci U S A*. 2009;106(12):4917–4922.
15. Majumdar S, et al. Truncated G protein-coupled mu opioid receptor MOR-1 splice variants are targets for highly potent opioid analgesics lacking side effects. *Proc Natl Acad Sci U S A*. 2011;108(49):19778–19783.
16. Lu Z, Xu J, Rossi GC, Majumdar S, Pasternak GW, Pan YX. Mediation of opioid analgesia by a truncated 6-transmembrane GPCR. *J Clin Invest*. 2015;125(7):2626–2630.
17. Xu J, et al. Stabilization of the μ-opioid receptor by truncated single transmembrane splice variants through a chaperone-like action. *J Biol Chem*. 2013;288(29):21211–21227.
18. Pan YX, Xu J, Mahurter L, Xu M, Gilbert AK, Pasternak GW. Identification and characterization of two new human mu opioid receptor splice variants, hMOR-1O and hMOR-1X. *Biochem Biophys Res Commun*. 2003;301(4):1057–1061.
19. Xu J, et al. Differential expressions of the alternatively spliced variant mRNAs of the μ opioid receptor gene, OPRM1, in brain regions of four inbred mouse strains. *PLoS One*. 2014;9(10):e111267.
20. Pan YX, et al. Isolation and expression of a novel alternatively spliced mu opioid receptor isoform, MOR-1F. *FEBS Lett*. 2000;466(2–3):337–340.
21. Xu J, et al. Stabilization of morphine tolerance with long-term dosing: association with selective upregulation of mu-opioid receptor splice variant mRNAs. *Proc Natl Acad Sci U S A*. 2015;112(1):279–284.
22. Abbadie C, Pan Y, Drake CT, Pasternak GW. Comparative immunohistochemical distributions of carboxy terminus epitopes from the mu-opioid receptor splice variants MOR-1D, MOR-1 and MOR-1C in the mouse and rat CNS. *Neuroscience*. 2000;100(1):141–153.
23. Abbadie C, Pasternak GW, Aicher SA. Presynaptic localization of the carboxy-terminus epitopes of the [mu] opioid receptor splice variants MOR-1C and MOR-1D in the superficial laminae of the rat spinal cord. *Neuroscience*. 2001;106(4):833–842.
24. Liu XY, et al. Unidirectional cross-activation of GRPR by MOR1D uncouples itch and analgesia induced by opioids. *Cell*. 2011;147(2):447–458.
25. Pan YX, et al. Identification and characterization of three new alternatively spliced mu-opioid receptor isoforms. *Mol Pharmacol*. 1999;56(2):396–403.
26. Pasternak DA, et al. Identification of three new alternatively spliced variants of the rat mu opioid receptor gene: dissociation of affinity and efficacy. *J Neurochem*. 2004;91(4):881–890.
27. Pan L, Xu J, Yu R, Xu MM, Pan YX, Pasternak GW. Identification and characterization of six new alternatively spliced variants of the human mu opioid receptor gene, Oprm. *Neuroscience*. 2005;133(1):209–220.
28. Koch T, Schulz S, Schröder H, Wolf R, Raulf E, Höllt V. Carboxyl-terminal splicing of the rat mu opioid receptor modulates agonist-mediated internalization and receptor resensitization. *J Biol Chem*. 1998;273(22):13652–13657.
29. Tanowitz M, von Zastrow M. A novel endocytic recycling signal that distinguishes the membrane trafficking of naturally occurring opioid receptors. *J Biol Chem*. 2003;278(46):45978–45986.
30. Kest B, Hopkins E, Palmese CA, Adler M, Mogil JS. Genetic variation in morphine analgesic tolerance: a survey of 11 inbred mouse strains. *Pharmacol Biochem Behav*. 2002;73(4):821–828.
31. Kest B, Palmese CA, Hopkins E, Adler M, Juni A, Mogil JS. Naloxone-precipitated withdrawal jumping in 11 inbred mouse strains: evidence

for common genetic mechanisms in acute and chronic morphine physical dependence. *Neuroscience*. 2002;115(2):463–469.
32. Klein G, Juni A, Waxman AR, Arout CA, Inturrisi CE, Kest B. A survey of acute and chronic heroin dependence in ten inbred mouse strains: evidence of genetic correlation with morphine dependence. *Pharmacol Biochem Behav*. 2008;90(3):447–452.
33. Hall FS, et al. Congenic C57BL/6 mu opiate receptor (MOR) knockout mice: baseline and opiate effects. *Genes Brain Behav*. 2003;2(2):114–121.
34. Schuller AG, et al. Retention of heroin and morphine-6 beta-glucuronide analgesia in a new line of mice lacking exon 1 of MOR-1. *Nat Neurosci*. 1999;2(2):151–156.
35. Kolesnikov Y, Jain S, Wilson R, Pasternak GW. Lack of morphine and enkephalin tolerance in 129/SvEv mice: evidence for a NMDA receptor defect. *J Pharmacol Exp Ther*. 1998;284(2):455–459.
36. Dockstader CL, Van der Kooy D. Mouse strain differences in opiate reward learning are explained by differences in anxiety, not reward or learning. *J Neurosci*. 2001;21(22):9077–9081.
37. Murphy NP, Lam HA, Maidment NT. A comparison of morphine-induced locomotor activity and mesolimbic dopamine release in C57BL6, 129Sv and DBA2 mice. *J Neurochem*. 2001;79(3):626–635.
38. Creese I, Snyder SH. Receptor binding and pharmacological activity of opiates in the guinea-pig intestine. *J Pharmacol Exp Ther*. 1975;194(1):205–219.
39. Rossi GC, Pan YX, Brown GP, Pasternak GW. Antisense mapping the MOR-1 opioid receptor: evidence for alternative splicing and a novel morphine-6 beta-glucuronide receptor. *FEBS Lett*. 1995;369(2-3):192–196.
40. VanderWende C, Spoerlein MT. Morphine-induced catalepsy in mice. Modification by drugs acting on neurotransmitter systems. *Neuropharmacology*. 1979;18(7):633–637.
41. Zarrindast MR, Samadi P, Haeri-Rohani A, Moazami N, Shafizadeh M. Nicotine potentiation of morphine-induced catalepsy in mice. *Pharmacol Biochem Behav*. 2002;72(1-2):197–202.
42. Williams JT, et al. Regulation of μ-opioid receptors: desensitization, phosphorylation, internalization, and tolerance. *Pharmacol Rev*. 2013;65(1):223–254.
43. Raehal KM, Schmid CL, Groer CE, Bohn LM. Functional selectivity at the μ-opioid receptor: implications for understanding opioid analgesia and tolerance. *Pharmacol Rev*. 2011;63(4):1001–1019.
44. Gainetdinov RR, Premont RT, Bohn LM, Lefkowitz RJ, Caron MG. Desensitization of G protein-coupled receptors and neuronal functions. *Annu Rev Neurosci*. 2004;27:107–144.
45. Qiu Y, Law PY, Loh HH. Mu-opioid receptor desensitization: role of receptor phosphorylation, internalization, and representation. *J Biol Chem*. 2003;278(38):36733–36739.
46. Zheng H, Loh HH, Law PY. β-Arrestin-dependent mu-opioid receptor-activated extracellular signal-regulated kinases (ERKs) translocate to nucleus in contrast to G protein-dependent ERK activation. *Mol Pharmacol*. 2008;73(1):178–190.
47. Kenakin T, Watson C, Muniz-Medina V, Christopoulos A, Novick S. A simple method for quantifying functional selectivity and agonist bias. *ACS Chem Neurosci*. 2012;3(3):193–203.
48. van der Westhuizen ET, Breton B, Christopoulos A, Bouvier M. Quantification of ligand bias for clinically relevant β2-adrenergic receptor ligands: implications for drug taxonomy. *Mol Pharmacol*. 2014;85(3):492–509.
49. Xu J, Xu M, Bolan E, Gilbert AK, Pasternak GW, Pan YX. Isolating and characterizing three alternatively spliced mu opioid receptor variants: mMOR-1A, mMOR-1O, and mMOR-1P. *Synapse*. 2014;68(4):144–152.
50. Snyder SH, Pasternak GW. Historical review: opioid receptors. *Trends Pharmacol Sci*. 2003;24(4):198–205.
51. Katritch V, Fenalti G, Abola EE, Roth BL, Cherezov V, Stevens RC. Allosteric sodium in class A GPCR signaling. *Trends Biochem Sci*. 2014;39(5):233–244.
52. Pert CB, Pasternak G, Snyder SH. Opiate agonists and antagonists discriminated by receptor binding in brain. *Science*. 1973;182(4119):1359–1361.
53. Enquist J, Kim JA, Bartlett S, Ferwerda M, Whistler JL. A novel knock-in mouse reveals mechanistically distinct forms of morphine tolerance. *J Pharmacol Exp Ther*. 2011;338(2):633–640.
54. Sim-Selley LJ, et al. Region-dependent attenuation of mu opioid receptor-mediated G-protein activation in mouse CNS as a function of morphine tolerance. *Br J Pharmacol*. 2007;151(8):1324–1333.
55. Sim LJ, Selley DE, Dworkin SI, Childers SR. Effects of chronic morphine administration on m opioid receptor- stimulated [35S]GTPgamaS autoradiography in rat brain. *J Neurosci*. 1996;16(8):2684–2692.
56. Bohn LM, Gainetdinov RR, Lin FT, Lefkowitz RJ, Caron MG. Mu-opioid receptor desensitization by beta-arrestin-2 determines morphine tolerance but not dependence. *Nature*. 2000;408(6813):720–723.
57. Bohn LM, Lefkowitz RJ, Caron MG. Differential mechanisms of morphine antinociceptive tolerance revealed in (beta)arrestin-2 knock-out mice. *J Neurosci*. 2002;22(23):10494–10500.
58. Raehal KM, Bohn LM. The role of β-arrestin2 in the severity of antinociceptive tolerance and physical dependence induced by different opioid pain therapeutics. *Neuropharmacology*. 2011;60(1):58–65.
59. Raehal KM, Walker JK, Bohn LM. Morphine side effects in β-arrestin 2 knockout mice. *J Pharmacol Exp Ther*. 2005;314(3):1195–1201.
60. Bohn LM, et al. Enhanced rewarding properties of morphine, but not cocaine, in beta(arrestin)-2 knock-out mice. *J Neurosci*. 2003;23(32):10265–10273.
61. Bohn LM, Lefkowitz RJ, Gainetdinov RR, Peppel K, Caron MG, Lin FT. Enhanced morphine analgesia in mice lacking b-arrestin 2. *Science*. 1999;286(5449):2495–2498.
62. Mann A, Illing S, Miess E, Schulz S. Different mechanisms of homologous and heterologous μ-opioid receptor phosphorylation. *Br J Pharmacol*. 2015;172(2):311–316.
63. Lau EK, et al. Quantitative encoding of the effect of a partial agonist on individual opioid receptors by multisite phosphorylation and threshold detection. *Sci Signal*. 2011;4(185):ra52.
64. Grecksch G, et al. Analgesic tolerance to high-efficacy agonists but not to morphine is diminished in phosphorylation-deficient S375A μ-opioid receptor knock-in mice. *J Neurosci*. 2011;31(39):13890–13896.
65. Deng HB, et al. Role for the C-terminus in agonist-induced mu opioid receptor phosphorylation and desensitization. *Biochemistry*. 2000;39(18):5492–5499.
66. Wolf R, et al. Replacement of threonine 394 by alanine facilitates internalization and resensitization of the rat mu opioid receptor. *Mol Pharmacol*. 1999;55(2):263–268.
67. Wang XF, et al. T394A mutation at the μ opioid receptor blocks opioid tolerance and increases vulnerability to heroin self-administration in mice. *J Neurosci*. 2016;36(40):10392–10403.
68. Xue Y, Zhou F, Zhu M, Ahmed K, Chen G, Yao X. GPS: a comprehensive www server for phosphorylation sites prediction. *Nucleic Acids Res*. 2005;33(Web Server issue):W184–W187.
69. Kang Y, et al. Crystal structure of rhodopsin bound to arrestin by femtosecond X-ray laser. *Nature*. 2015;523(7562):561–567.
70. Pan YX, Xu J, Xu M, Rossi GC, Matulonis JE, Pasternak GW. Involvement of exon 11-associated variants of the mu opioid receptor MOR-1 in heroin, but not morphine, actions. *Proc Natl Acad Sci U S A*. 2009;106(12):4917–4922.
71. Matthes HWD, et al. Loss of morphine-induced analgesia, reward effect and withdrawal symptoms in mice lacking the m-opioid-receptor gene. *Nature*. 1996;383(6603):819–823.
72. Sora I, et al. Opiate receptor knockout mice define mu receptor roles in endogenous nociceptive responses and morphine-induced analgesia. *Proc Natl Acad Sci U S A*. 1997;94(4):1544–1549.
73. Loh HH, Liu HC, Cavalli A, Yang W, Chen YF, Wei LN. mu Opioid receptor knockout in mice: effects on ligand-induced analgesia and morphine lethality. *Brain Res Mol Brain Res*. 1998;54(2):321–326.
74. Zhou H, et al. A novel morpholino oligomer targeting ISS-N1 improves rescue of severe spinal muscular atrophy transgenic mice. *Hum Gene Ther*. 2013;24(3):331–342.
75. Widrick JJ, Jiang S, Choi SJ, Knuth ST, Morcos PA. An octaguanidine-morpholino oligo conjugate improves muscle function of mdx mice. *Muscle Nerve*. 2011;44(4):563–570.
76. Zhou H, Meng J, Marrosu E, Janghra N, Morgan J, Muntoni F. Repeated low doses of morpholino antisense oligomer: an intermediate mouse model of spinal muscular atrophy to explore the window of therapeutic response. *Hum Mol Genet*. 2015;24(22):6265–6277.
77. Yokota T, et al. Extensive and prolonged restoration of dystrophin expression with vivo-morpholino-mediated multiple exon skipping in dystrophic dogs. *Nucleic Acid Ther*. 2012;22(5):306–315.
78. Douglas AG, Wood MJ. Splicing therapy for neuromuscular disease. *Mol Cell Neurosci*. 2013;56:169–185.
79. Suwanmanee T, et al. Restoration of human beta-globin gene expression in murine and human IVS2-654 thalassemic erythroid cells by free uptake of antisense oligonucleotides. *Mol Pharmacol*. 2002;62(3):545–553.
80. Kole R, Krainer AR, Altman S. RNA therapeutics: beyond RNA interference and antisense oligonucleotides. *Nat Rev Drug Discov*. 2012;11(2):125–140.